GCSM
11th Global Conference on Sustainable Manufacturing
2013
23rd - 25th September
Berlin - Germany

8.2 Finite element modeling of laser assisted friction stir welding of carbon steels for enhanced sustainability of welded joints

A. H. Kheireddine, A. H. Ammouri, R. F. Hamade

Department of Mechanical Engineering, American University of Beirut (AUB), Beirut, Lebanon

Abstract

In Friction stir welding (FSW) of carbon steels, process parameters must be set to avoid defects such as warm holes. Proper selection of process parameters also affects the final grain microstructure and phase transformations and, ultimately, the weld's mechanical properties. Process parameters, including laser-assisted heating, of AISI 1045 carbon steel were investigated via a 3D finite element method (FEM) model. The laser action was modeled as heat source with constant flux. The simulation findings favorably agree with experiments reported in the literature and suggesting that with laser-assisted-FSW welding can be performed at higher traverse speeds (400 vs. 100 mm/min) while maintaining defect free weld. Also, evolved phase transformations are predicted across the weld geometry as time progresses. Such findings will help in the prediction of sound welding parameters and in estimating the mechanical properties of the various regions of the weld leading to more sustainable joints.

Keywords:
FEM; Simulations, Friction stir welding; Laser.

1 INTRODUCTION

Friction stir welding (FSW) is a solid state joining process that utilizes a rapidly-rotating, high strength steel tool in the form of a pin inserted along the weld steam to join similar or dissimilar metals. Known problems associated with friction stir welding (FSW) may be alleviated by the proper selection of process parameters leading to more sustainable processing and to enhanced welded joints. Such parameters include tool feed, spindle speed, tool geometry, tool tilt angle, and in-process cooling or heating. The proper selection of such factors is a key for achieving defect-free welds by avoiding defects such as warm holes and voids. Furthermore, achieving desirable grain size at the weld as well as the final phases also results from the combination of the process parameters which must be carefully defined in order to achieve target results.

FSW is considered a hot-working process in which massive plastic deformation occurs through the rotating pin without subjecting the workpiece to any form of induced heating or melting. Such deformation gives rise to a thermomechanically-affected rejoin (TMAZ) and a heat-affected zone (HAZ) [1]. During the welding process, the material is wiped from the front side of the pin onto the back side in a helical motion within the stir zone [2]. Among the advantages of Friction stir welding is the ability of this technique to efficiently control the cooling rate and peak temperature by varying the speed of the rotating pin [3]. FSW is used in joining metals of poor weldability and in many green applications [4]. Friction stir welding is heavily used in the aerospace industry to join, for example, high strength aluminum alloys that are hard to weld using traditional welding techniques. For steel and other high-temperature materials, the application of FSW is limited to the presence of suitable tools that can operate in the temperature range of 1000 to 1200 °C [5]. This is due to the fact that the heat produced by stirring and friction may not be sufficient to soften the material around the rotating tool. Therefore, it is important to select tool materials with good wear resistance and toughness at temperatures of 1000°C or higher [4]. However, in the past few years, studies have reported to the effect that FSW is capable of achieving grain improvements in the stir zone in steels similar to those observed in light metals such as aluminum. A number of studies that tackle microstructural changes during FSW have been conducted to examine the influence of the welding parameters on material flow and the shape of the interface between the various zones. One such study [6] modeled friction stir welding of stainless steel (304L) utilizing the finite element method (FEM) and using an Eulerian formulation with coupled viscoplastic flow and heat transfer around the tool pin. Some of the findings were that: higher temperatures on the advancing side compared to the retreating side, higher strength in the weld zone compared to the base material, harder friction stirred zones compared to the unreformed base metals, highest effective stress in the stirred zone, more anisotropy in the material near the friction stirred zone than the material passing farther from the tool pin. The microstructure and mechanical properties of welded joints are significantly affected by such parameters as heat input during welding, the composition of steel metal used, and the in-process cooling and heating of the welded zone [7]. In-process laser heating was introduced in [8] where a laser beam was used as a preheating source during friction stir welding. Preheating in this process aids in softening the metal before stirring and thus increasing the speed of the rotating tool and less work is now required by the tool to raise the temperature of the workpiece. Using this technique the heat generated by the tool is reduced and the tool life is increased. Moreover, the higher rotational speeds and the higher cooling rates attained (above 600 mm/min) by laser-assisted FSW prevented the formation of brittle martensite which increases the hardness of the welded zone [9]. For more sustainable laser-assisted friction stir welding processes, the process will have to capture some of the elements defined in [10] to characterize sustainability: (1) power consumption, (2) operational safety, (3) personnel health, (4) environmental impact, (5) manufacturing costs and (6) waste management.

G. Seliger (Ed.), Proceedings of the 11th Global Conference on Sustainable Manufacturing - Innovative Solutions
ISBN 978-3-7983-2609-5 © Universitätsverlag der TU Berlin 2013

Although laser assisted FSW requires higher power inputs but with preheating higher production rates can be achieved thus decreasing the total production costs. Moreover, it is believed that achieving a better quality product especially through enhancing surface integrity is a main aspect of manufacturing sustainability. Using preheating in FSW through laser beam was found [11] to enhance surface integrity through increasing the surface hardness via refined microstructure evolution. In addition to that the approach followed which is numerical simulation for optimization purposes is proven to decrease costs relative to experimental approaches. In this paper, a finite element model was developed to simulate the Laser-assisted FSW and optimize the process parameters to enhance surface integrity and microstructural properties which affect the tool ware resistance and as a result the sustainability of the process. The commercial modelling software DEFORM-3D™ (Scientific Forming Technologies Corporation, 2545 Farmers Drive, Suite 200, Columbus, Ohio 43235) was used as a fully thermo-mechanically coupled FE model to simulate the process. The model accounted for phase transformation taking place and was validated against experimental data.

2 THE FEM MODEL

2.1 Parts and Meshes

A thermo-mechanically coupled model using the FE software DEFORM was implemented to model the friction stir welding of carbon steel. As shown in figure 1, the model comprises the tool, the workpiece, and the backing plate. Also shown superimposed on the meshed geometry is a rendering of the in-process laser source. To model the laser source, a heat source circular window with constant heat flux was defined. The circular window is of diameter 2 mm and is placed 5 mm in front of the tool. The power of the laser was 2kW.

Both the tool and the backing plate were modeled as rigid un-deformable bodies where only heat transfer was accounted. On the other hand the workpiece was modeled as a plastic body subject to deformation and heat. The two plates to be welded were modeled as one block to avoid numerical instabilities at the contact.

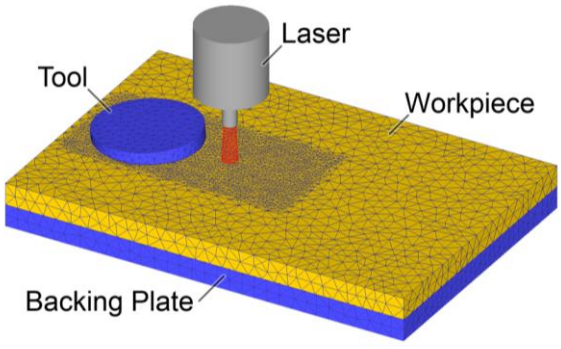

Figure 1: The meshed FE model showing the tool, workpiece, and backing plate (under the workpiece). Shown superimposed is a rendering of the in-process laser source.

The considered tool was a cylindrical shoulder 15mm in diameter. From the bottom of the shoulder, a 6 mm diameter smooth unthreaded pin extrudes 3.2 mm. The tool was tilted 3° about the vertical axis in the processing direction to further improve material flow. Both the workpiece and the backing plate had an area of 60x40 mm2 and a thickness of 3.2 mm.

Tetrahedral elements were used in the FEM model. The tool and the backing plate were meshed for thermal analysis purposes only with each containing around 10000 and 5000 elements respectively while the workpiece had around 24000 elements. To further capture the state variables at the tool-workpiece interface, a rectangular mesh control window was applied around the processing area of interest where finer mesh elements (around 0.3 mm) were created as shown in Figure 6.

2.2 Material Modeling

The material used for the tool and the backing plate was WC based alloy. As for the workpiece, it is believed that the final weld mechanical properties are strictly dependent on the volume fraction of phases present. Therefore, AISI 1045 (workpiece material) was defined as a mixture of phases. Specifically three phases were defined: martensite, austenite, and pearlite. The transformation to any of the phases was defined according phase transformation, isothermal, and continuous cooling transformation diagrams. The functions recommended by DEFORM are listed below in Table 1 and which were used along with the appropriate generated latent heat values. The initial volume fraction of the elements was defined as 100 percent pearlite which is predominatly the case of as received mild-carbon steels. Each phase has its own materiel properties which are, in turn, function of temperature. Similarly, each of the phases has its own flow stress equation. The linear hardening equation used to formulate the stress equation was

$$\bar{\sigma} = \mathrm{Y}(\mathrm{T},\mathrm{A}) + \mathrm{H}(\mathrm{T},\mathrm{A})\bar{\varepsilon} \quad (1)$$

where,

A = Atom content

T = Temperature

$\bar{\varepsilon}$ = Effective plastic strain

$\bar{\sigma}$ = Flow stress

Y = Initial yield stress (temperature dependent)

H = Strain hardening (temperature dependent)

Table 1: Phase Transformation Models

Phase 1	Phase 2	Transformation Model
Austenite	Martensite	Magee's Equation
Austenite	Pearlite	Diffusion(TTT curve)
Martensite	Austenite	Diffusion(Simplified)
Pearlite	Austenite	Diffusion(Simplified)

2.3 Friction Modeling

Friction at the tool-workpiece interface is a very complex process due to the variation of temperature, strain rate, and stress which make friction modeling a difficult task. In [12] a numerical model with experimental evidence was developed to estimate the shear friction coefficient in FSW. The model uses the tool speed and dimensions to estimate the shear friction coefficient as shown below:

$$\mu f = \mu 0 \exp(-\lambda \delta \omega r) \quad (2)$$

where δ is the percentage sticking and r is the radial distance from the tool axis for the point in consideration. The values used were as follows: μ0= 0.4, δ= 0.4, ω=62.8 radians, r= 0.003m and constant λ was 1s/m [12].

2.4 Boundary Conditions

Heat transfer with the environment was accounted for the three meshed objects (tool, workpiece, and backing plate) via a convective heat coefficient of 20 W/(m2 ºC) at a constant temperature set at 293K for the surrounding environment. The heat transfer coefficient between the tool-workpiece and the backing plate-workpiece interfaces was set to 11 kW/(m2ºC). Local re-meshing was triggered by a relative interference ratio of 70% between contacting edges. This would ensure the integrity of the workpiece geometry during deformation. The simulation time step selection should be optimized to prevent redundant calculations while preserving the state variables' accuracy. The time step in the simulation was determined based on the tool rotational speed and the minimum element size to guarantee a calculation step every 5 degrees of the tool rotation. Simulation time was further reduced by neglecting the plunging phase of FSW and taking into consideration the traversing phase alone. The tool final plunged shape was cut from the workpiece geometric model to account for the deformation produced by the plunging phase. A dwelling phase was added at the beginning of each run where the tool spins in its place to raise the temperature at the stir zone to the plunging elevated levels. In tool movement definition, a trapezoidal speed profile with a rise time of 0.5s was used. This would ensure a smooth processing start and prevent voids during the plunging stage.

3 MODEL VALIDATION

The FEM model was validated against experimental data available in the literature by tracking the temperature history of an observation point at the seam line at a distance of 0.5 mm above the shoulder for two different test cases. The processing parameters of both cases are described in table 2.

Table 2: Processing parameters of the validation test cases

Property	Case 1	Case 2
Rotational speed (RPM)	600	600
Traverse speed (mm/min)	100	400

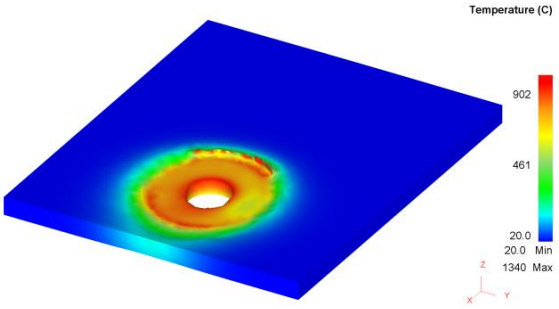

Figure 2: Temperature contour plot in workpiece for case 2 (rotational spindle speed = 600 rpm, traverse speed = 400 mm/min) after 6 seconds of welding

Figure 2 shows the temperature contours for case 2 (rotational spindle speed = 600 rpm, traverse speed = 400 mm/min) where peak temperature is located at the pin/tool interface as one would normally expect in an FSW process.

Plotted in Figure 3 are the simulated temperature profiles versus time for 2 cases: normal FSW and laser-assisted FSW. Co-plotted are the peak temperatures measured in [8]. It can be seen from the Figure that the peak simulated temperature is very close to the experimentally measured maximum temperature for case 2 for both cases: normal FSW and in-process laser assisted FSW.

Another comparison is made in Figure 4 where the peak temperatures for rotational spindle speed = 600 rpm are plotted against traverse speed at 100 and 400 mm/min. Although the peak temperatures are not exactly matching between experimental and numerical aproaches, the differences in both cases are less than 16% and a similar trend of decreasing temperature with increasing advancing speed is reached. Figures 3 and 4 constitute the model validation phase in this work.

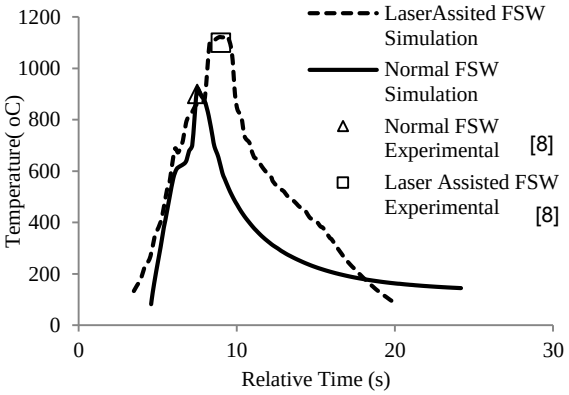

Figure 3: Simulation temperature profile with experimental [8] peak temperature for case 2 (rotational spindle speed = 600 rpm).

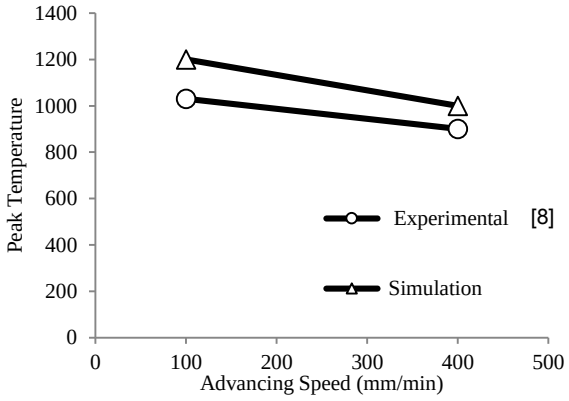

Figure 4: Peak temperatures versus advancing speed for experimental [8] and simulation test cases (rotational spindle speed = 600 rpm).

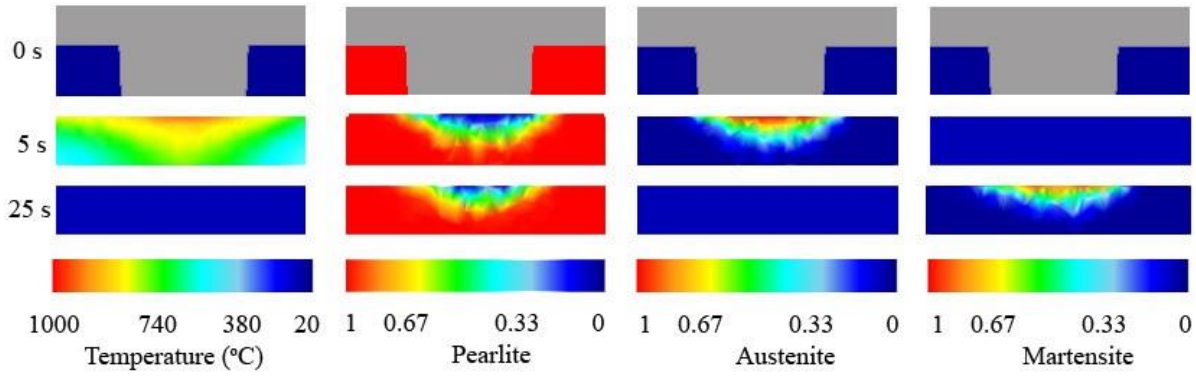

Figure 5: Phase transformation with time as the tool moves away for the normal friction stir welding (RPM=600; V=400 mm/min)

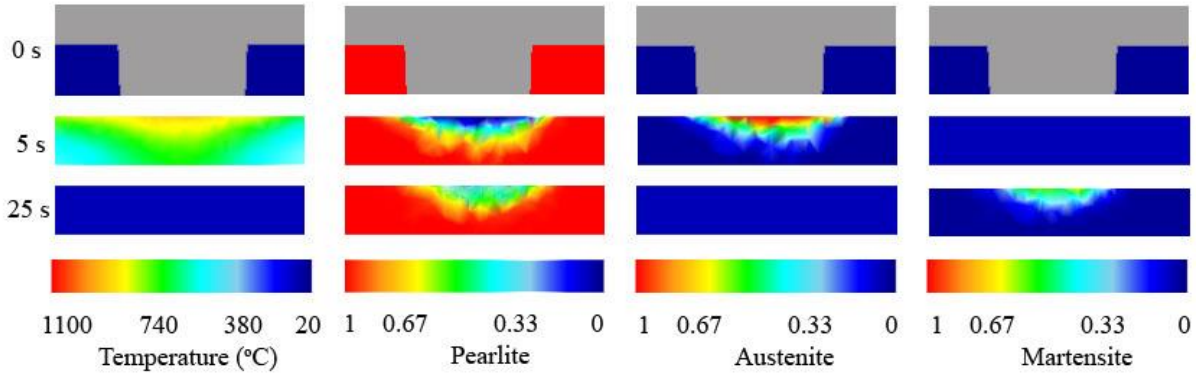

Figure 6: Phase transformation with time as tool moves away for laser assisted friction stir welding (RPM=600; V=400 mm/min)

4 RESULTS

4.1 Phase transformations

The resulting mechanical properties of carbon steel joints ultimately depend on the intermetallic phases present and, thus, on the heating and cooling histories during the process. During FSW of carbon steels, temperature exceeds the transition temperature (about 727 °C for many steels) at which austenite begins to form upon heating. Therefore, transformations form austenite to other forms such as pearlite, martensite, and bainite will take place afterwards. Furthermore, the amount and type of these transformations is directly affected by the maximum temperature (mostly related to rotational speed) and cooling rate (mostly related to advancing speed). Other external heating (e.g., laser) and cooling (cryogenic) sources during FSW/FSP also play a critical role in altering these phase transformations and the resulting grain size for many materials [13,14].

In this work, modeling of phase transformations was made possible in DEFORM by defining a material subject to steel phase transformations according to the scenarios listed in Table 1. To illustrate, a section at the pin center was considered and the history of temperature with corresponding phases as the pin moves away was monitored (Figure 5, left). From Figure 5, it is clear that after exceeding 727°C pearlite starts to transform into austenite specifically at the stir zone. Then, after reaching the maximum temperature at about 5 seconds, the cooling stage starts. In the cooling stage, some of the austenite transforms to martensite and some transform back to pearlite. This formation of martensite was reported using a transmission electron microscope, TEM, by [8] while using the same processing parameters. It is also worth mentioning that from Figures 5 and 6 one can notice that larger phase transformations take place at the advancing side as compared with the receding side. This may be expected given that larger deformations take place at that side compared with the receding side and, thus, resulting in higher temperatures (heating and cooling).

4.2 Effect of In-process Laser Heating

The application of laser increases the maximum temperature during FSW as shown in Figure 6 by about 100°C compared to normal FSW. This increase in temperature slowed the cooling rate which is believed to be behind martensite formation. The formation of brittle martensite in FSW joints is usually avoided. Therefore, in order to enhance the weld hardness, and thus weld sustainability, some may add pre-heating sources to lower the cooling rate thus reducing martensite formation. Laser-assisted heating was found to be a suitable method used to aid in the heating the joint during FSW steel joining [8]. Moreover, with laser-assisted FSW, higher weld speeds can be achieved increasing the productivity and, thus, process and product sustainability. Contrasting Figure 5 with Figure 6, one can notice that less pearlite is transformed to martensite during in laser-assisted FSW. This is expected because of the lower cooling rate with the application of laser and also because more time is spent while cooling from higher peak temperatures.

5 SUMMARY AND CONCLUSIONS

An FEM model was developed to simulate the in-process laser assisted friction stir welding of AISI 1045 carbon steel.

The simulation results of peak temperatures of the weld were validated against experimental work reported by other researchers [8]. The effect of advancing speed on weld temperature was examined where peak temperatures were found to decrease with increasing traverse welding speed. With laser assistance, however, higher welding temperatures can now be reached faster at higher welding speeds thus increasing the sustainability of the process. Furthermore, the resulting phase transformations, which have direct effect on the microstructure and, thus, the mechanical properties of the weld were successfully accounted in the model. It was found that with laser-assisted processing, smaller phase fraction of the brittle martensite phase is formed at the stir zone resulting in enhanced properties of the welded joint and, thus, enhancing weld sustainability. It is believed that such model can be used for optimization purposes leading to more sustainable processes and, more importantly, sustainable products.

6 ACKNOWLEDGMENTS

This publication was made possible by the National Priorities Research Program (NPRP) grant # 09-611-2-236 from the Qatar National Research Fund (a member of The Qatar Foundation). The statements made herein are solely the responsibility of the authors. The second author gratefully acknowledges the support of Consolidated Contractors Company (CCC) through the CCC Doctoral Fellowship in Manufacturing.

7 REFERENCES

[1]. K.V. Jata and S.L. Semiatin. 2000. Continues dynamic recrystallization during friction stir welding of high strength aluminum alloys. *Scripta mater* 43 (2000) 743-749.

[2]. M. Guerra, C. Schmidt, J.C. McClure, L.E. Murr, A.C. Nunes, 2002. Flow patterns during friction stir welding. *Materials Characterization* 49 (2003) 95–101.

[3]. L. Cui, H. Fujii, N. Tsuji, K. Nogi.2007. Friction stir welding of a high carbon steel. *Scripta Materialia* 56 (2007) 637–640.

[4]. R. Mishra, Z. Ma. 2005. Friction stir welding and processing. Materials *Science and Engineering* R 50 (2005) 1–78.

[5]. A. Ozekcin, H. Jin, J. Koo, N. Bangaru, R. Ayer. 2004. A Microstructural Study of Friction Stir Welded Joints of Carbon Steels. *International Journal of Offshore and Polar Engineering*.

[6]. J Cho, Donald E. Boyce, P. Dawson. 2005. Modeling strain hardening and texture evolution in friction stir welding of stainless steel. *Materials Science and Engineering* A 398 (2005) 146–163.

[7]. H. Fujii, L. Cui, N. Tsuji, M. Maeda, K. Nakata, K. Nogi.2006. Friction stir welding of carbon steels. *Materials Science and Engineering* A 429 (2006) 50–57.

[8]. Y. Sun, Y. Konishi, M. Kamai, H. Fujii. Microstructure and mechanical properties of S45C steel prepared by laser-assisted friction stir welding. *Materials and Design* 47 (2013) 842–849. Ueji R, Fujii H, Cui L, Nishioka A, Kunishige K, Nogi K. Friction stir welding of ultrafine grained plain low-carbon steel formed by the Martensite process. Mater Sci Eng A 2006;423(1–2):324–30

[9]. Jawahir, I.S. and Dillon, O.J., 2007, Sustainable Manufacturing Processes: New Challenges for Developing Predictive Models and Optimization Techniques, (Keynote Paper), Proc. 1st International Conference on Sustainable Manufacturing (SM1), Montreal, Canada, October 18-19, 2007, pp. 1-19.

[10]. Jawahir, I.S, Brinksmeier, E., M'Saoubi, R., Aspinwall, D.K., Outerio, J.C., Meyer, D., Umbrello, D., Jayal, A.D., 2011, Surface Integrity in material removal process: Recent Advances, CIRP Annals – Manufacturing Technology, 60:603-626.

[11]. Buffa, G., Fratini, L., and Shivpuri, R., 2007, "CDRX Modelling in Friction Stir Welding of AA7075-T6 Aluminum Alloy: Analytical Approaches," Journal of Materials Processing Technology, 191(1-3) pp. 356-359.

[12]. Nandan, R., Prabu, B., De, A., & Debroy, T., 2007, Improving reliability of heat transfer and materials flow calculations during friction stir welding of dissimilar aluminum alloys. WELDING JOURNAL-NEWYORK-, 86(10), 313.

[13]. A.H. Kheireddine, A. H. Ammouri, R. F. Hamade, G. T. Kridli, 2012, FEM analysis of the effects of cooling techniques on the microstructure of aluminum 7075 friction stir welded joints, IMECE2012-88943, proceedings of the ASME 2012 International Mechanical Engineering Congress & Exposition, IMECE2012, November 9-15, 2012, Houston, Texas, USA

[14]. A. H. Ammouri, A. H. Kheireddine, R. F. Hamade, G. T. Kridli, 2013, FEM optimization of process parameters and in-process cooling in the friction stir processing of magnesium alloy az31b, IMECE2013-62468, ASME 2013 International Mechanical Engineering Congress & Exposition, IMECE2013, Nov 15-21, 2013, San Diego, USA.